

Scaling behavior of the spin pumping effect in ferromagnet/platinum bilayers

F. D. Czeschka,¹ L. Dreher,² M. S. Brandt,² M. Weiler,¹ M. Althammer,¹ I.-M. Imort,³ G. Reiss,³ A. Thomas,³ W. Schoch,⁴ W. Limmer,⁴ H. Huebl,¹ R. Gross,^{1,5} and S. T. B. Goennenwein^{1,*}

¹*Walther-Meißner-Institut, Bayerische Akademie der Wissenschaften, 85748 Garching, Germany*

²*Walter Schottky Institut, Technische Universität München, 85748 Garching, Germany*

³*Fakultät für Physik, Universität Bielefeld, 33602 Bielefeld, Germany*

⁴*Institut für Quantenmaterie, Universität Ulm, 89069 Ulm, Germany*

⁵*Physik-Department, Technische Universität München, 85748 Garching, Germany*

We systematically measured the DC voltage V_{ISH} induced by spin pumping together with the inverse spin Hall effect in ferromagnet/platinum bilayer films. In all our samples, comprising ferromagnetic $3d$ transition metals, Heusler compounds, ferrite spinel oxides, and magnetic semiconductors, V_{ISH} invariably has the same polarity, and scales with the magnetization precession cone angle. These findings, together with the spin mixing conductance derived from the experimental data, quantitatively corroborate the present theoretical understanding of spin pumping in combination with the inverse spin Hall effect.

Spin current related phenomena are an important aspect of modern magnetism [1–4]. For example, pure spin currents – a directed flow of angular momentum without an accompanying net charge current – can propagate in magnetic insulators [5]. A spin current \mathbf{J}_s can be detected via the inverse spin Hall (ISH) effect, where \mathbf{J}_s with polarization orientation $\hat{\mathbf{s}}$ is converted into a charge current $\mathbf{J}_c \propto \alpha_{\text{SH}} (\hat{\mathbf{s}} \times \mathbf{J}_s)$ perpendicular to both $\hat{\mathbf{s}}$ and \mathbf{J}_s [2, 6]. Recently, Mosendz *et al.* [7] showed that the spin Hall angle α_{SH} can be quantitatively determined from so-called spin pumping experiments in ferromagnet/normal metal (F/N) bilayers. Here, the magnetization of the F layer is driven into ferromagnetic resonance (FMR) and can relax by emitting a spin current into the adjacent N layer [8, 9]. Spin pumping can thus be understood as the inverse of spin torque [1, 10], and gives access to the physics of spin currents, magnetization dynamics, and damping. The present theoretical models [8, 11] suggest that spin pumping in conductive ferromagnets is a generic phenomenon, where the magnitude of \mathbf{J}_s is governed by the magnetization precession cone angle and the spin mixing conductance $g_{\uparrow\downarrow}$ at the F/N interface. However, most spin pumping experiments to date have been performed in transition metals [9, 12, 13], so that generic properties could not be addressed. In this letter, we provide experimental evidence that the present theories for spin pumping are not limited to transition metal-based bilayers, but also apply to the ferromagnetic Heusler compounds Co_2FeAl and Co_2FeSi , the ferrimagnetic oxide spinel Fe_3O_4 , and the dilute magnetic semiconductor (Ga,Mn)As (DMS). We demonstrate this by simultaneous DC voltage and FMR measurements that yield the correlation of the inverse spin Hall voltage $V_{\text{ISH}} \propto J_c$ along \mathbf{J}_c and the magnetization precession cone angle Θ in FMR. Our experimental findings clearly confirm the scaling behavior of V_{ISH} suggested by theory.

We fabricated F/Pt bilayers, using Ni, Co, Fe, Co_2FeAl , Co_2FeSi , Fe_3O_4 , and (Ga,Mn)As, for the F layer. The Ni, Co and Fe films were deposited on oxi-

dized silicon substrates via electron beam evaporation at a base pressure of 1×10^{-8} mbar. The Heusler compounds were sputtered on (001)-oriented MgO single crystal substrates at an Ar pressure of 1.5×10^{-3} mbar, followed by annealing at 500°C [14]. Epitaxial (100)- and (111)-oriented Fe_3O_4 films were grown via pulsed laser deposition in argon atmosphere on (100)-oriented MgO and (0001)-oriented Al_2O_3 substrates, respectively, at a substrate temperature of 320°C [15]. The $\text{Ga}_{1-x}\text{Mn}_x\text{As}$ ($x = 0.04$) films were grown via low temperature molecular beam epitaxy on (001)-oriented GaAs substrates [16]. All F layers have a thickness $t_F = 10$ nm, except for the (111)-oriented Fe_3O_4 film, which has $t_F = 35$ nm, and the (Ga,Mn)As films with $t_F = 200$ nm, 175 nm and 65 nm. As a high-quality, transparent interface is crucial for spin pumping [17], all F layers were covered in situ with $t_N = 7$ nm of Pt, except for the (Ga,Mn)As films, which were covered after exposure to ambient atmosphere. All samples were cut into rectangular bars (length $L = 3$ mm, width $w = 1$ mm or 2 mm) and contacted on the short sides for electrical measurements as shown in Fig. 1(a).

The FMR and spin pumping experiments were performed in a magnetic resonance spectrometer at a fixed microwave frequency $\nu_{\text{MW}} = 9.3$ GHz as a function of an externally applied static magnetic field \mathbf{H} , in the temperature range from 2 K to 290 K. We took care to position the respective sample on the axis of the TE_{102} microwave cavity, in order to locate it in an antinode of the microwave magnetic field and in a node of the microwave electric field. The FMR was recorded using magnetic field modulation and lock-in detection, so that the resonance field H_{res} corresponds to the inflection point in the FMR spectra. The DC voltage V_{DC} between the contacts indicated in Fig. 1(a) was measured with a nanovoltmeter.

Figure 1 shows a selection of FMR and V_{DC} spectra, recorded for two magnetic field orientations in the film plane: $\phi = 0^\circ$ corresponds to \mathbf{H} parallel to $\hat{\mathbf{x}}$ (black

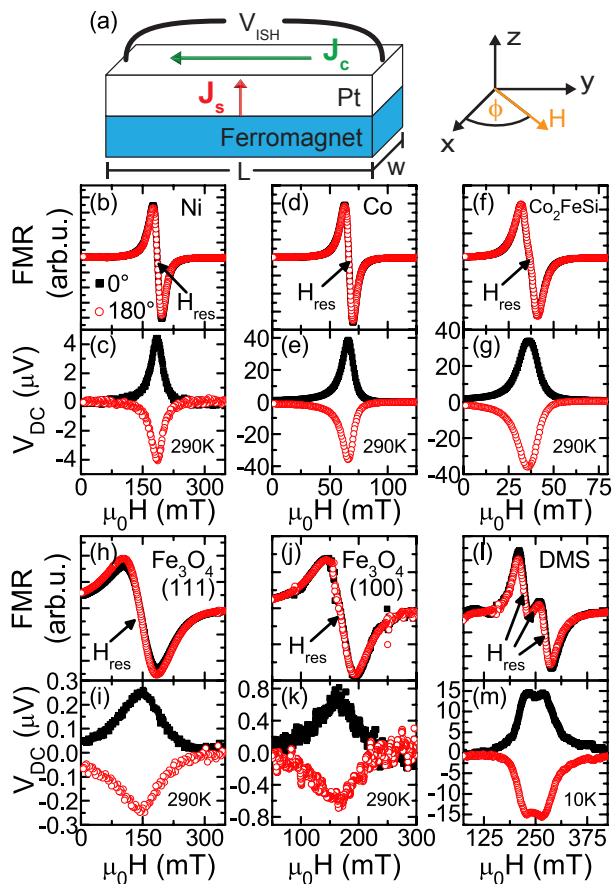


FIG. 1. (a) Sketch of the the coordinate system and the F/Pt bilayer sample. (b),(d),(f),(h),(j),(l) show the FMR signal of F/Pt bilayers, with F as quoted in the individual panels, recorded with \mathbf{H} parallel (black full squares) and antiparallel (red open circles) to \hat{x} . DMS stands for 200 nm (Ga,Mn)As. (c),(e),(g),(i),(k),(m) show the DC voltage measured simultaneously with the respective FMR traces.

full squares), while for $\phi = 180^\circ$, \mathbf{H} is antiparallel to \hat{x} (red open circles). All measurements in Fig. 1 were taken at 290 K, except for the (Ga,Mn)As data recorded at $T = 10$ K (Fig. 1(l) and (m)). Since the FMR is invariant with respect to magnetic field inversion, the FMR traces for $\phi = 0^\circ$ and $\phi = 180^\circ$ should superimpose, as indeed observed in experiment. The FMR signal of all samples in Fig. 1 consists of a single resonance line, with the exception of (Ga,Mn)As, in which several standing spin wave modes contribute to the FMR spectrum [18]. The V_{DC} traces show one clear extremum in V_{DC} at H_{res} ; only in (Ga,Mn)As, several V_{DC} extrema corresponding to the spin wave modes can be discerned. The magnitude of V_{DC} ranges from a few 100 nV in Fe_3O_4 to a few 10 μV in Co_2FeSi and Fe (Fig. 2). In contrast to the FMR, the V_{DC} extremum changes sign when the magnetic field is reversed. It also is important to note that V_{DC} always has a maximum ($V_{DC} > 0$) for $\phi = 0^\circ$, whereas a minimum ($V_{DC} < 0$) is observed for $\phi = 180^\circ$.

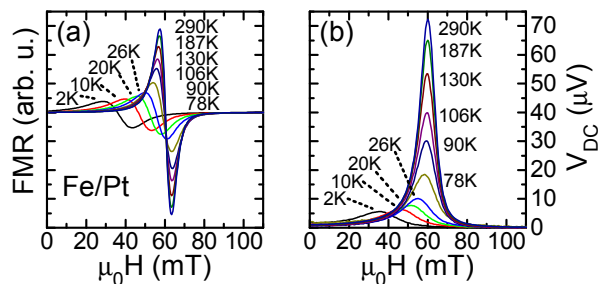


FIG. 2. Temperature-dependent evolution of (a) the FMR, and (b) the V_{DC} spectra of a Fe/Pt bilayer.

We furthermore studied the evolution of the FMR and V_{DC} signals as a function of temperature in several bilayer samples. As an example, the FMR and V_{DC} spectra of an Fe/Pt sample, recorded for a series of temperatures $2\text{ K} \leq T \leq 290\text{ K}$ are shown in Fig. 2. With decreasing T , the FMR broadens and shifts to lower H_{res} , as does the peak in V_{DC} .

We now turn to the interpretation of the experimental data of Figs. 1 and 2. We attribute the peaks in V_{DC} to spin pumping in combination with the inverse spin Hall effect in the F/Pt bilayers [7–9]. This naturally explains that V_{DC} changes sign when the \mathbf{H} orientation is inverted from $\phi=0^\circ$ to 180° , as \mathbf{H} determines the orientation of the spin polarization vector \hat{s} in $\mathbf{J}_c \propto (\hat{s} \times \mathbf{J}_s)$. Hence, \mathbf{J}_c and thus also V_{DC} is reversed if the magnetic field is inverted. We note that the H_{res} are well above the coercive and the anisotropy fields of the respective ferromagnets, such that the magnetization $\mathbf{M} \parallel \mathbf{H}$ in good approximation. Furthermore, the experimental observation that V_{DC} invariably has the same polarity for a given field orientation ϕ , irrespective of the ferromagnetic material used in the F/Pt bilayer and of the measurement temperature, is fully consistent with spin pumping theory [7, 8, 11, 19–21]. We note that other mechanisms for the generation of a DC voltage in conjunction with FMR have been suggested and were observed in experiment [22–24]. Microwave rectification effects linked to the anisotropic magnetoresistance or the anomalous Hall effect often are superimposed onto the spin pumping signal, in particular if the sample is not located in a node of the microwave electric field [7, 25]. However, we rule out such mechanisms as the origin of the V_{DC} observed in our experiments (Figs. 1 and 2) for two reasons. First, we have positioned the sample in a node of the microwave electric field, which minimizes rectification-type processes. Second, and more importantly, both the spontaneous resistivity anisotropy $\Delta\rho$ determining the anisotropic magnetoresistance and the anomalous Hall coefficient R_H are substantially different in magnitude and in sign for the different ferromagnetic materials in our F/Pt bilayers [26]. Nevertheless, for a given ϕ , we invariably observe the same V_{DC} polarity, which is diffi-

cult to rationalize for rectification effects.

In order to quantitatively compare our experimental data with spin pumping theory, we start from

$$V_{\text{ISH}} = \frac{-e \alpha_{\text{SH}} \lambda_{\text{SD}} \tanh \frac{t_{\text{N}}}{2\lambda_{\text{SD}}}}{\sigma_{\text{F}} t_{\text{F}} + \sigma_{\text{N}} t_{\text{N}}} g_{\uparrow\downarrow} \nu_{\text{MW}} L P \sin^2 \Theta \quad (1)$$

derived by Mosendz *et al.* [7, 21] for the inverse spin Hall DC voltage V_{ISH} arising due to spin pumping in permalloy/N bilayers, assuming that the N layer is an ideal spin current sink. Here, e is the electron charge, λ_{SD} is the spin diffusion length in N, $g_{\uparrow\downarrow}$ is the effective spin mixing conductance [21], Θ is the magnetization precession cone angle (cf. inset in Fig. 3(a)), and P is a correction factor taking into account the ellipticity of the magnetization precession [21, 27]. For our samples, we calculated $0.5 \leq P \leq 1.3$. Note that Eq. (1) has been adapted to our experimental configuration, and accounts for both the conductivity σ_{N} and σ_{F} of the N and F layer contributing to the bilayer conductivity.

Since invariably $t_{\text{N}} = 7$ nm and N=Pt for all our bilayer samples, $C \equiv \alpha_{\text{SH}} \lambda_{\text{SD}} \tanh(t_{\text{N}}/2\lambda_{\text{SD}})$ is a constant at a given temperature. In addition, the denominator in Eq. (1) can be expressed in terms of the sample geometry w/L and resistance R , measured in four point experiments: $\sigma_{\text{F}} t_{\text{F}} + \sigma_{\text{N}} t_{\text{N}} = (Rw/L)^{-1}$. We thus rewrite Eq. (1) as

$$\frac{V_{\text{ISH}}}{\nu_{\text{MW}} P R w} = -e C g_{\uparrow\downarrow} \sin^2 \Theta. \quad (2)$$

The theoretical models for the spin mixing conductance [11, 28] suggest that $g_{\uparrow\downarrow}$ of conductive ferromagnet/normal metal interfaces is determined mainly by the N layer, i.e., the Pt layer in our case. In other words, $g_{\uparrow\downarrow}$ should be of comparable magnitude in all our samples. Equation (2) then represents a scaling relation for all F/Pt bilayers made from a conductive ferromagnet and a Pt layer of one and the same thickness t_{N} , irrespective of the particular ferromagnetic material, its magnetic properties, or the details of the charge transport mechanism such as band conduction or charge carrier hopping.

We now test the scaling relation of Eq. (2) against our experimental data. At ferromagnetic resonance, the magnetization precession cone angle is $\Theta_{\text{res}} = 2h_{\text{MW}}/(\sqrt{3}\Delta H_{\text{pp}})$ [30], with the microwave magnetic field $h_{\text{MW}} = 0.12$ mT as determined in paramagnetic resonance calibration experiments. We extract the FMR peak-to-peak line width ΔH_{pp} from the experimental data, and use the measured DC voltage $V_{\text{DC, res}}$ at H_{res} to determine $V_{\text{ISH}} = V_{\text{DC, res}}$. Figure 3(a) shows $V_{\text{ISH}}/(\nu_{\text{MW}} P R w)$ versus $\sin^2 \Theta_{\text{res}}$ thus obtained. Full symbols indicate data measured at 290 K, while measurements at lower temperatures are shown as open symbols. Data for permalloy/Pt (Py/Pt) extracted from Refs. [7, 21, 29] are also included in the figure. For the sake of completeness, data for $\text{Y}_3\text{Fe}_5\text{O}_{12}/\text{Pt}$ (YIG/Pt),

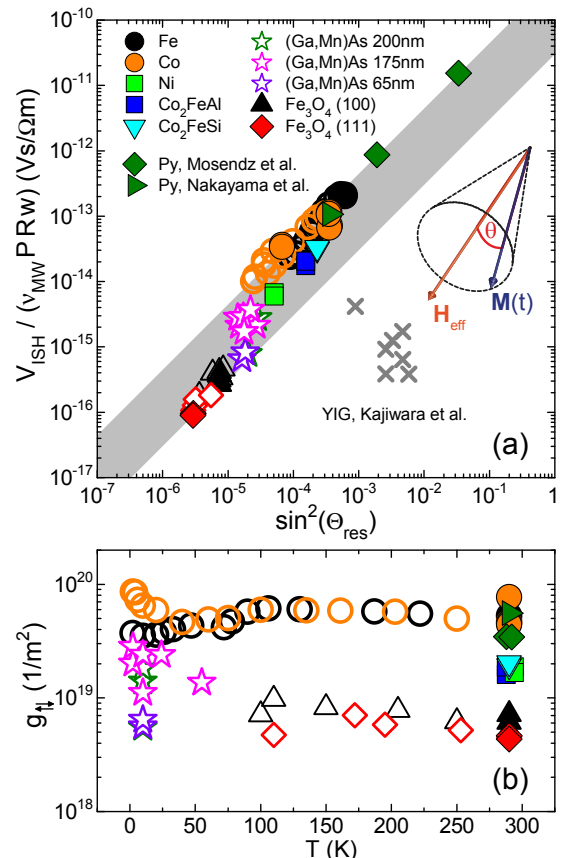


FIG. 3. (a) In all F/Pt bilayers made from conductive ferromagnets, the DC voltage V_{ISH} induced by a collective mode FMR scales with $\sin^2 \Theta_{\text{res}}$ to within a factor of 10, as indicated by the grey bar. The inset depicts the magnetization precession around the effective magnetic field. (b) From the scaling analysis, the spin mixing conductance $g_{\uparrow\downarrow}$ can be quantified as a function of temperature (see text). In panels (a) and (b), full symbols represent data taken at 290 K, open symbols correspond to data measured at lower T . The Py and YIG data are taken from the literature, Refs. [5, 7, 21, 29].

taken from Ref. [5], are also shown. Since YIG is an insulator, however, $g_{\uparrow\downarrow}$ is dominated by its imaginary part, in contrast to the mostly real $g_{\uparrow\downarrow}$ for conductive ferromagnets [11, 31, 32]. Moreover, spin wave modes govern the YIG FMR signal, impeding a straightforward analysis [33]. Thus, we here focus only on conductive ferromagnet/Pt bilayers. In these samples, $V_{\text{ISH}}/(\nu_{\text{MW}} P R w)$ indeed scales as suggested by Eq. (2) to within a factor of 10 (grey bar in Fig. 3(a)). The deviations from perfect scaling are due to a slight material dependence of $g_{\uparrow\downarrow}$, as detailed in the next paragraph. The scaling behavior is observed over more than four orders of magnitude in $V_{\text{ISH}}/(\nu_{\text{MW}} P R w)$ and $\sin^2 \Theta_{\text{res}}$, for samples made from conductive ferromagnetic films with qualitatively different exchange mechanisms, transport properties, crystalline quality, and crystalline structure. Moreover, F/N bilayer samples fabricated and investigated by

different groups are consistently described.

To quantify $g_{\uparrow\downarrow}$ of a given bilayer, we write Eq. (2) as $g_{\uparrow\downarrow} = -V_{\text{SH}} / [\nu_{\text{MW}} P R w e C \sin^2 \Theta_{\text{res}}]$. Using the room temperature values $\alpha_{\text{SH}} = 0.013$ and $\lambda_{\text{SD}} = 10$ nm for Pt [21, 34], P calculated as detailed in Ref. [21] (and literature values for the conductivities of Py and Pt [7, 35] for the data points extracted from Refs. [7, 21, 29]), we obtain $g_{\uparrow\downarrow}$ as shown in Fig. 3(b). Clearly, the conjecture that $g_{\uparrow\downarrow}$ is independent of the F layer properties is well fulfilled for highly conductive (“metallic”) ferromagnets, such as the 3d transition metals, permalloy, or the Heusler compounds, which all are in the range $g_{\uparrow\downarrow} = (4 \pm 3) \times 10^{19} \text{ m}^{-2}$. In the low-conductivity ferromagnet Fe_3O_4 , $g_{\uparrow\downarrow}$ is about a factor of 6 smaller, but the linear scaling is still observed. In (Ga,Mn)As, $g_{\uparrow\downarrow}$ appears to be in between these two regimes. However, several spin wave modes contribute to the FMR in (Ga,Mn)As (cf. Fig. 1(l)) and a fit with at least three Lorentzian lines was required to reproduce the FMR and V_{DC} data. So the assumption of a single, position-independent magnetization precession cone angle Θ_{res} is not warranted [18]. For standing spin waves, the magnetization precession amplitude $\Theta_{\text{res}}(z)$ changes as a function of z across the film thickness, which in turn can qualitatively alter the magnitude of V_{DC} [33]. Since $\Theta_{\text{res}}(z)$ moreover depends on the particular spin wave mode excited, a more thorough study of spin pumping due to spin wave modes is mandatory to evaluate $g_{\uparrow\downarrow}$ in (Ga,Mn)As/Pt. In addition, in systems with large spin-orbit coupling such as (Ga,Mn)As, the magnetization precession can even induce a charge current via an inverse, spin-orbit driven spin torque effect [36]. Taken together, the experimental results summarized in Fig. 3(b) represent an incentive to theory to calculate $g_{\uparrow\downarrow}$ for ferromagnets with different conductivity magnitude, transport mechanisms, and inhomogeneous spin texture.

Another interesting experimental observation from Fig. 3(b) is that temperature has little influence on $g_{\uparrow\downarrow}$. According to the present theoretical understanding, $g_{\uparrow\downarrow}$ in diffusive bilayers is governed by the conductivity $\sigma_{\text{N}}(T)$ of the normal metal [11, 28]. The weak temperature dependence of $g_{\uparrow\downarrow}$ (Fig. 3(b)) thus suggests that $\sigma_{\text{N}}(T)$ of our Pt films also should not substantially change with temperature. This is corroborated by resistance measurements, which show that $\sigma_{\text{N}}(T)$ increases by less than a factor of 2 from 290 K to 2 K. Since $\alpha_{\text{SH}} \propto \sigma^{0.6\dots 1}$ [34, 37] is governed by $\sigma_{\text{N}}(T)$, and since λ_{SD} in Pt increases by less than 50% from 290 K to 2 K [34], $C = \alpha_{\text{SH}} \lambda_{\text{SD}} \tanh(t_{\text{N}}/2\lambda_{\text{SD}})$ changes by at most a factor of 3 in the whole temperature range investigated experimentally. This warrants the use of $Cg_{\uparrow\downarrow}$ as an essentially temperature-independent scaling constant in Eq. (2).

In summary, we have measured the DC voltage caused by spin pumping and the inverse spin Hall effect in F/Pt samples, with F made from elemental 3d ferromagnets, the ferromagnetic Heusler compounds Co_2FeAl

and Co_2FeSi , the ferrimagnetic oxide spinel Fe_3O_4 , and the magnetic semiconductor (Ga,Mn)As. Although the magnetic exchange mechanism, the saturation magnetization, the spin polarization, the charge carrier transport mechanism and the charge carrier polarity are qualitatively different in the different samples, the DC voltage has identical polarity for all bilayers investigated, and its magnitude is well described by a scaling relation of the form of Eq. (2) within the entire temperature range $2 \text{ K} \leq T \leq 290 \text{ K}$ studied. Our experimental findings thus quantitatively corroborate the present spin pumping/inverse spin Hall theories [7, 8, 11, 19–21], and are an incentive for quantitative calculations of $g_{\uparrow\downarrow}(T)$ in various types of F/N bilayers.

We thank G. E. W. Bauer for valuable discussions. The work at WMI was financially supported via the Excellence Cluster “Nanosystems Initiative Munich (NIM)”. A.T. and I.-M. I. are supported by the NRW MIWF.

* goennenwein@wmi.badw.de

- [1] D. C. Ralph and M. D. Stiles, *J. Magn. Magn. Mater.* **320**, 1190 (2008).
- [2] S. Takahashi and S. Maekawa, *Sci. Technol. Adv. Mat.* **9**, 014105 (2008).
- [3] I. Zutic, J. Fabian, and S. D. Sarma, *Rev. Mod. Phys.* **76**, 323 (2004).
- [4] S. Maekawa, *Concepts in Spin Electronics* (Oxford University Press, New York, 2006).
- [5] Y. Kajiwara *et al.*, *Nature* **464**, 262 (2010).
- [6] J. E. Hirsch, *Phys. Rev. Lett.* **83**, 1834 (1999).
- [7] O. Mosendz *et al.*, *Phys. Rev. Lett.* **104**, 046601 (2010).
- [8] Y. Tserkovnyak, A. Brataas, and G. E. W. Bauer, *Phys. Rev. B* **66**, 224403 (2002).
- [9] E. Saitoh *et al.*, *Appl. Phys. Lett.* **88**, 182509 (2006).
- [10] J. A. Katine *et al.*, *Phys. Rev. Lett.* **84**, 3149 (2000).
- [11] Y. Tserkovnyak, A. Brataas, and G. E. W. Bauer, *Phys. Rev. Lett.* **88**, 117601 (2002).
- [12] R. Urban, G. Woltersdorf, and B. Heinrich, *Phys. Rev. Lett.* **87**, 217204 (2001).
- [13] M. Costache *et al.*, *Phys. Rev. Lett.* **97**, 216603 (2006).
- [14] D. Ebke *et al.*, *J. Magn. Magn. Mater.* **322**, 996 (2010).
- [15] D. Venkateshvaran *et al.*, *Phys. Rev. B* **79**, 134405 (2009).
- [16] W. Limmer *et al.*, *Phys. Rev. B* **74**, 205205 (2006).
- [17] O. Mosendz *et al.*, *Appl. Phys. Lett.* **96**, 022502 (2010).
- [18] C. Bihler *et al.*, *Phys. Rev. B* **79**, 045205 (2009).
- [19] Y. Tserkovnyak *et al.*, *Rev. Mod. Phys.* **77**, 1375 (2005).
- [20] X. Wang *et al.*, *Phys. Rev. Lett.* **97**, 216602 (2006).
- [21] O. Mosendz *et al.*, *Phys. Rev. B* **82**, 214403 (2010).
- [22] W. G. Egan and H. J. Juretschke, *J. Appl. Phys.* **34**, 1477 (1963).
- [23] Y. S. Gui, N. Mecking, and C.-M. Hu, *Phys. Rev. Lett.* **98**, 217603 (2007).
- [24] N. Mecking, Y. S. Gui, and C.-M. Hu, *Phys. Rev. B* **76**, 224430 (2007).
- [25] H. Y. Inoue *et al.*, *J. Appl. Phys.* **102**, 083915 (2007).
- [26] R. C. O’Handley, *Modern Magnetic Materials : Principles and Applications* (John Wiley, New York, 2000).

- [27] K. Ando, T. Yoshino, and E. Saitoh, Appl. Phys. Lett. **94**, 152509 (2009).
- [28] A. Brataas, Y. V. Nazarov, and G. E. W. Bauer, Phys. Rev. Lett. **84**, 2481 (2000).
- [29] H. Nakayama *et al.*, IEEE Trans. Magn. **46**, 2202 (2010).
- [30] Y. Guan *et al.*, J. Magn. Magn. Mater. **312**, 374 (2007).
- [31] K. Xia *et al.*, Phys. Rev. B **65**, 220401 (2002).
- [32] K. Carva and I. Turek, Phys. Rev. B **76**, 104409 (2007).
- [33] C. W. Sandweg *et al.*, Appl. Phys. Lett. **97**, 252504 (2010).
- [34] L. Vila, T. Kimura, and Y. Otani, Phys. Rev. Lett. **99**, 226604 (2007).
- [35] K. Ando *et al.*, Phys. Rev. Lett. **101**, 036601 (2008).
- [36] K. M. D. Hals, A. Brataas, and Y. Tserkovnyak, Europhys. Lett. **90**, 47002 (2010).
- [37] H. Nakayama *et al.*, J. Phys: Conf. Ser. **200**, 062014 (2010).